JTTEE5 21:480–488
DOI: 10.1007/s11666-012-9761-2
1059-9630/$19.00 © ASM International

Peer-Reviewed

Comparison of the Microstructural Characteristics and Electrical Properties of Thermally Sprayed Al_2O_3 Coatings from Aqueous Suspensions and Feedstock Powders

Filofteia-Laura Toma, Lutz-Michael Berger, Stefan Scheitz, Stefan Langner, Conny Rödel, Annegret Potthoff, Viktar Sauchuk, and Mihails Kusnezoff

(Submitted September 16, 2011; in revised form January 23, 2012)

In this work the microstructural characteristics and electrical insulating properties of thermally sprayed alumina coatings produced by suspension-HVOF (S-HVOF) and conventional HVOF spray processes are presented. The electrical resistance at different relative air humidity (RH) levels (from 6 to 97% RH) and values of dielectric strength were investigated by direct current electrical resistance measurements, electrochemical impedance spectroscopy, and dielectric breakdown tests. Relationships between electrical properties and coating characteristics are discussed. At low humidity levels (up to 40% RH) the electrical resistivities of S-HVOF and HVOF coatings were on the same order of magnitude (10^{11} Ω·m). At a very high humidity level (97% RH) the electrical resistivity values for the S-HVOF coatings were in the range 10^{7}-10^{11} Ω·m, up to five orders of magnitude higher than those recorded for the HVOF coating (orders of magnitude of 10^{6} Ω·m). The better electrical resistance stability of the suspension-sprayed Al_2O_3 coatings can be explained by their specific microstructure and retention of a higher content of α-Al_2O_3. The dielectric strength E_d of suspension-sprayed coatings was found to be 19.5-26.8 kV·mm^{-1} for coating thicknesses ranging from 60 to 200 μm. These values were slightly lower than those obtained for conventional HVOF coatings (up to 32 kV·mm^{-1}). However, it seemed that the dielectric strength of conventionally sprayed coatings was more sensitive to the coating thickness (when compared with the values of E_d determined for S-HVOF coatings) and varied to a greater extent (up to 10 kV·mm^{-1}) when the coating thickness varied in the range 100-200 μm.

Keywords Al_2O_3, dielectric strength, electrical resistivity, HVOF, microstructure, phases, suspension

1. Introduction

Thermally sprayed alumina coatings with suitable dielectric properties have been prepared and tested for the manufacturing of electrostatic chucks, discharge devices, and insulating coatings for high-temperature heaters (Ref 1-5). Compared with sintered alumina, which consists solely of the thermodynamically stable α-Al_2O_3 (corundum), thermally sprayed coatings contain mainly metastable phases (γ- and δ-alumina), even though all commonly used feedstock spray powders consist of α-Al_2O_3. The properties of the metastable phases differ significantly from those of corundum; the stronger reaction of γ-alumina with water or water vapour presumably has a negative effect on the dielectric properties of the material. It is generally agreed that coatings consisting primarily of α-Al_2O_3 are desirable.

In a previous work by the authors (Ref 6) the electrical insulating properties of alumina coatings produced by conventional APS and HVOF spray processes were described. From the direct current (DC) electrical resistance and electrochemical impedance spectroscopy (EIS) measurements it was shown that at low relative air humidity (RH) levels the values of electrical resistivity were around 10^{11} Ω·m for both the APS coatings and the HVOF alumina coatings with a higher content of α-Al_2O_3. In humid environments the presence of α-Al_2O_3 is expected to play an important role in the retention of electrical properties. At high humidity levels (>75% RH) the electrical resistance values obtained for HVOF alumina coatings were greater

This article is an invited paper selected from presentations at the 2011 International Thermal Spray Conference and has been expanded from the original presentation. It is simultaneously published in *Thermal Spray 2011: Proceedings of the International Thermal Spray Conference*, Hamburg, Germany, September 27-29, 2011, Basil R. Marple, Arvind Agarwal, Margaret M. Hyland, Yuk-Chiu Lau, Chang-Jiu Li, Rogerio S. Lima, and André McDonald, Ed., ASM International, Materials Park, OH, 2011.

Filofteia-Laura Toma, Lutz-Michael Berger, Stefan Scheitz, and **Stefan Langner**, Fraunhofer Institute for Material and Beam Technology (Fh-IWS), Winterbergstrasse 28, 01277 Dresden, Germany; and **Conny Rödel, Annegret Potthoff, Viktar Sauchuk,** and **Mihails Kusnezoff**, Fraunhofer Institute for Ceramic Technologies and Systems (Fh-IKTS), Winterbergstrasse 28, 01277 Dresden, Germany. Contact e-mail: filofteia-laura.toma@iws.fraunhofer.de.

than those obtained for APS coatings. The electrical resistivity decreased by approximately five orders of magnitude in very humid environments (97% RH) for both types of coatings. Moreover, both coating types showed no insulating behaviour (orders of magnitude of 10^6 Ω·m). A significant degradation in electrical properties (decrease in resistivity of nearly six orders of magnitude) with an increase in the air humidity (from 20 to 80% RH) was likewise noticed for α-Al_2O_3 powders (Ref 7). The deterioration of insulation properties with increasing humidity can be explained by the increase in surface electrical conductivity resulting from adsorption and accumulation of water monolayers on the oxide surface (Ref 8). Open pores and cracks in the coating microstructure should have a detrimental effect on the electrical properties. These coating imperfections can generate transverse channels in which capillary condensation of water vapour can occur, reducing the coating's electrical resistance.

Suspension thermal spraying and particularly suspension-HVOF (S-HVOF) spraying allow dense alumina coatings to be prepared from finely dispersed particles in aqueous or alcoholic suspensions (Ref 9-12). With appropriate selection of both the raw powder for suspension production and the spray parameters, thermal spraying with suspensions is an adequate method to produce mechanically stable alumina coatings consisting mainly of the α phase without using additives such as ceramic oxides (Ref 13). The suspension characteristics, i.e., raw material type and purity, particle sizes in suspension, and solid content, have a significant influence on the retention of α-Al_2O_3 (Ref 14). Suspension-sprayed alumina coatings show interesting mechanical and dry-sliding wear properties (Ref 9, 11, 12). However, little information is known about the electrical insulating properties of such coatings.

In this work a comparative study on the electrical resistance at different air humidity levels and dielectric strength values of alumina coatings produced by S-HVOF and HVOF processes was carried out. The coating characteristics of microstructure, crystalline phases, and mechanical properties are presented and the differences in electrical properties due to the different spray processes and coating characteristics are discussed.

2. Experimental Procedures

2.1 Materials and Deposition Processes

A commercially available fine alumina powder characterised by a very high purity (α-Al_2O_3, >99.99% Baikowski, La Balme de Sillingy, France) was used to produce an appropriate suspension for spraying. The raw powder contained submicron-sized grains, as depicted in the high-magnification SEM micrograph given in Fig. 1(a). The suspension was obtained by homogeneous dispersion of 35 wt.% solid in deionised water. Appropriate selection of the suspension pH and addition of a small quantity of an organic dispersion agent resulted in a highly stable aqueous suspension of low viscosity (around 3 mPa·s). The particle size distribution ($D_{90,3}$-$D_{10,3}$) in suspensions ranged from 0.4 to 3.5 μm and the average particle size was about 1.35 μm (Fig. 1b).

A commercial fused and crushed α-alumina powder (>99.7% purity, Ceram GmbH, Albbruck-Birndorf, Germany) with appropriate particle sizes for the HVOF process (−25 + 5 μm) was used to produce the conventionally sprayed coatings.

Both feedstock materials (suspension and powder) were sprayed with an HVOF TopGun (8-mm-diameter nozzle, GTV mbH, Germany) using ethylene as the fuel gas. A modified combustion chamber allowing internal injection of the suspension was adapted to the HVOF gun. Suspensions were fed from a pressurised vessel, as described in a previous work by the authors (Ref 10). The main spraying conditions for S-HVOF and HVOF processes are shown in Table 1. The spray parameters were selected for the preparation of dense alumina coatings. S-HVOF coatings with average thicknesses ranging from 60 to 200 μm were sprayed on grit-blasted copper plates (40 × 100 × 3 mm); HVOF coatings with average thicknesses of 100 and 200 μm were obtained on mild steel (30 × 30 × 3 mm). For evaluation of electrical properties at different air humidity levels, selected S-HVOF and

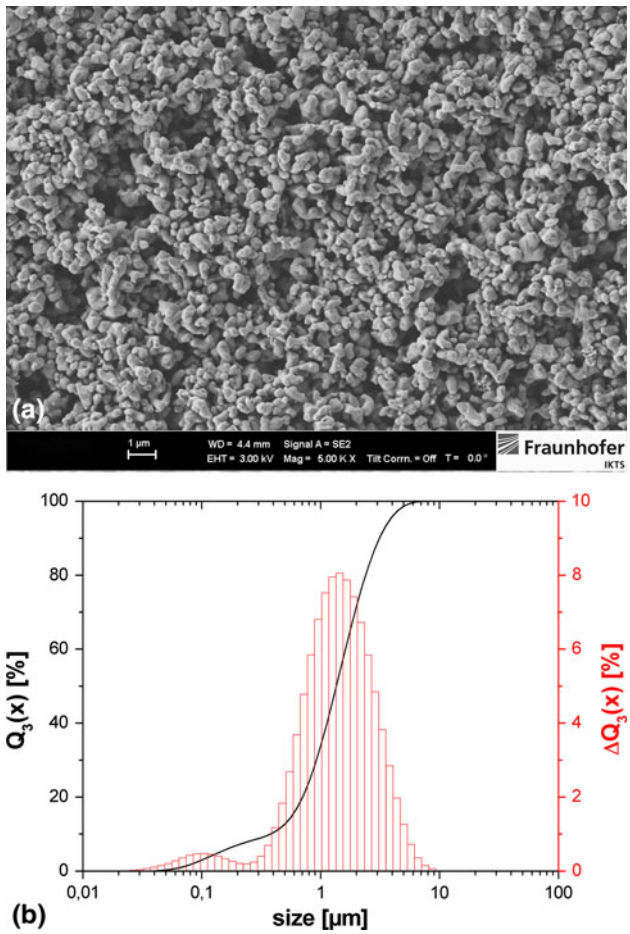

Fig. 1 (a) High-magnification SEM micrograph of fine alumina powder and (b) cumulative volume distribution of the particle in suspension

HVOF coatings were sprayed on highly corrosion-resistant 1.4462 stainless steel plates (60 × 100 × 5.5 mm). All the substrates had been previously grit blasted with EKF 54 corundum prior to spraying.

2.2 Coating Characterization

The coatings' microstructures were examined by optical microscopy and scanning electron microscopy on metallographically polished cross sections. The phase compositions were evaluated by x-ray diffraction using a D8 (Advance Bruker AXS) diffractometer. Measurements were carried out in the θ-2θ step scan mode using CuKα radiation and a step size of 0.05°. The phases were identified using the *Diffrac EVA software*. The content of crystalline α-Al_2O_3 (C_α) in the coatings was estimated using the following equation:

$$C_\alpha(\%) = \frac{A_\alpha(113)}{A_\alpha(113) + 0.89 \cdot A_\gamma(113)} \cdot 100$$

The coating roughness parameters R_a, R_z, and R_{max} were measured with a Mahr Perthometer (Mahr GmbH, Göttingen, Germany) using a tracing length $L_t = 17.5$ mm (total measured length $L_m = 12.5$ mm) and a cut-off $\lambda_c = 2.5$ mm. The Vickers microhardness HV0.3 (load of 2.94 N) was measured on the cross sections of 200-µm-thick coatings using an HP-Mikromat 1-HMV tester (Hegewald & Peschke Meß- und Prüftechnik GmbH, Nossen, Germany) with a load duration of 10 s. Young's modulus was determined on the cross sections using a Vickers micro-indenter (Shimadzu DUH-202 tester, Shimadzu Scientific Instruments) with a loading rate of 35 mN·s^{-1} and a holding time of 10 s at the load of 200 g (1.96 N). The Young's modulus values were extracted according to the Oliver-Pharr method (Ref 15).

2.3 Investigation of Electrical Insulation Properties

The insulation resistance and electrical resistivity of the coatings at room temperature and at different air humidity levels were investigated by DC measurements and the alternating current (AC) method, respectively. Dielectric breakdown tests were performed to evaluate the dielectric breakdown voltages (DBV) and dielectric strengths of the sprayed coatings.

The DC insulating resistance of the as-sprayed samples was measured using an Advantest R8340 Ultra-high Resistance Meter (Advantest Corporation, Tokyo, Japan) by applying DC voltages of 50, 100, and 200 V. Squares with areas from 10 × 20 mm^2 to 20 × 30 mm^2, depending on the sample geometries, were covered with silver paste to ensure the electrical contact. During application of the DC voltage the electrical contact was placed at a distance of about 2 mm from the edge of samples to avoid short-circuiting. For each voltage at least three measurements were performed and the average values of insulating resistance were determined.

The AC resistance/resistivity of the coatings was determined using the EIS technique. The EIS measurements were performed with a Zahner IM6 Impedance Analyser (Zahner-Elektrik GmbH & Co KG, Kronach, Germany) using a 2-electrode cell. A stainless steel electrode with a diameter of 3.5 cm was used as the counter electrode, whereas the coating specimen played the role of working electrode. An alternating voltage with an amplitude of 5 mV at zero DC bias in the frequency range from 1 MHz to 100 µHz was applied during the tests. EIS measurements were performed on as-sprayed suspension-sprayed coatings, whereas the conventional coatings were first ground (at a $R_a < 1$ µm) to provide a good contact and to reduce the influence of surface roughness.

For investigation of the influence of the RH on the electrical properties the samples were placed at room temperature in a desiccator and conditioned for long periods (from 48 h up to several days depending on the coating system) at different relative humidity levels ranging from 6% RH to 97% RH using saturated salt solutions. The resistance values were then determined by means of DC and EIS measurements using the same procedures as described above.

The dielectric breakdown tests were performed on as-sprayed coatings, without any surface finishing or sealing, at room temperature and room humidity (40-50% RH) through application of high DC voltages using a PC6P testmeter (Sefelec GmbH, Ottersweier, Germany). Electrodes 5 mm in diameter were used as electrical contacts for breakdown tests. The applied voltage was increased linearly at a rate of rise of 100 V·s^{-1} from zero up to the occurrence of flashover. A silver paste was applied to the coating surface to provide a good electrical contact. When the dielectric breakdown of the coating occurred the DBV was measured and the dielectric strength (E_d) was determined. The breakdown tests were applied on six or nine points on the coating surface of each sample and the average values of DBV and E_d were obtained.

Table 1 Main spray parameters

	Coating deposition	
Parameter	**S-HVOF**	**HVOF**
C_2H_4/O_2, L·min^{-1}	75/230	90/270
Spray distance, mm	80	150
Relative torch scan velocity, m·s^{-1}	1.6	1.6
Particle feed rate, g·min^{-1}	33-35	27-30
Scanning step size, mm	5	3
Substrate cooling during spray	Air jets	Air jets

3. Results

3.1 Microstructures and Phase Compositions

Both coating systems appeared to be dense in the optical micrographs given in Fig. 2, although the S-HVOF coatings showed a denser microstructure compared with their HVOF counterparts. High-magnification SEM micrographs revealed a specific microstructure (Fig. 3a and b) for the suspension-sprayed coatings differing from that of the conventionally sprayed coatings (Fig. 3c and d).

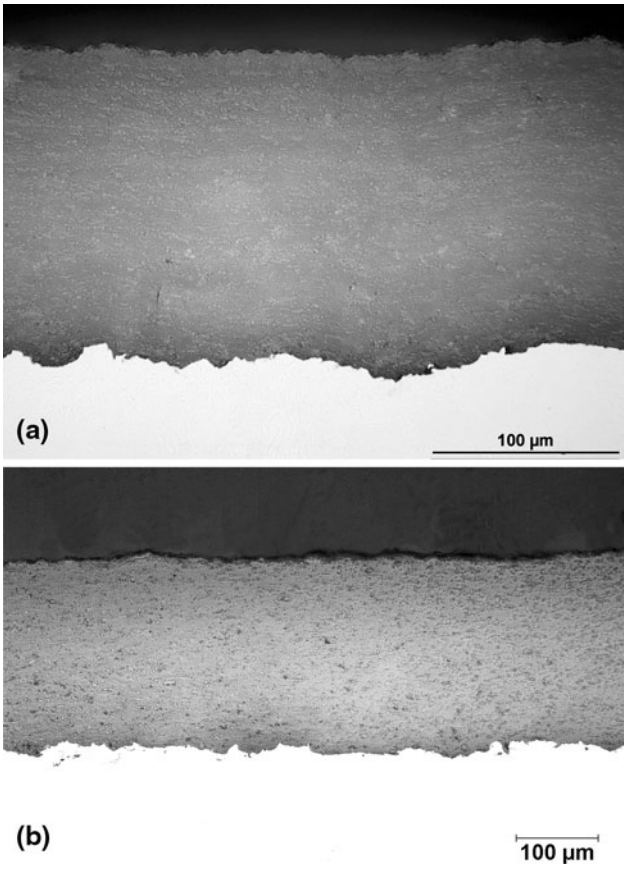

Fig. 2 Optical micrographs of alumina coatings obtained by (a) S-HVOF and (b) HVOF processes

Partially melted fine particles with elongated shapes (of about 5 µm in length and 150 nm in thickness), nearly spherical µm-sized particles and clusters of agglomerated tiny sub-µm-sized grains were embedded in the matrix of well-melted ones. The presence of small locally distributed vertical cracks (up to several tens of µm in length) and closed pores (with sizes ranging from about 100 nm to a few µm) could be detected in the SEM micrographs of the S-HVOF alumina coatings. These small vertical cracks most probably resulted from the very high thermal and relaxation stresses generated during the spraying process for the preparation of dense suspension-sprayed coatings. The HVOF coatings were characterised by the classic lamellar structure of thermally sprayed coatings consisting of well-melted and partially melted particles. The typical microstructural defects, inter- and intra-lamellar cracks, unmelted particles and pores, were also observed.

The XRD patterns for the sprayed coatings are shown in Fig. 4. The HVOF coating contained the metastable γ-Al_2O_3 phase (JCPDS card no. 10-0425) as the main phase and α-Al_2O_3 (JCPDS card no. 46-1212). Traces of β-Al_2O_3 (JCPDS card no. 10-0414) already identified in the feedstock powder (Ref 6) were also detected. In the S-HVOF alumina coating, the α-phase was the main crystalline phase. The content of α-phase was about 60% in the S-HVOF coating, whereas only 30% could be retained in the conventional HVOF coating.

3.2 Mechanical Properties

The microhardness values (750-850 HV0.3) and the Young's moduli (110-130 GPa; 1.96 N) obtained for the S-HVOF coatings were in the same range as those measured for conventional HVOF coatings (average microhardness: 820 ± 30 HV0.3, Young's modulus: 120 GPa (Ref 16)). Suspension spraying yielded smoother coating surfaces. Thus for S-HVOF coatings the values of R_a and R_z were about 2.4-3.5 and 15-22 µm, respectively, depending on the coating thickness, compared with R_a of 4.1-4.8 µm and R_z of 25-30 µm measured for conventional HVOF-sprayed coatings. The roughness values obtained in this work for the suspension coatings were significantly lower than those reported by Bolelli et al. (Ref 9).

3.3 Electrical Resistance Measurements

3.3.1 DC Resistance. DC insulating resistances for coatings with different thicknesses determined at room temperature in air at two different humidity levels (30-40% RH and 97% RH) are illustrated in Fig. 5. At comparable humidity levels the absolute values of resistance for each coating system were almost independent of the coating thickness. This was due to the fact that the size of the electrode was significantly greater than the coating thickness; consequently, the contact surface area influenced the resistance more than the coating thickness did. At a low humidity level the insulating resistance values for the S-HVOF sprayed coatings were determined to be 6.0×10^{10} Ω to 1.6×10^{11} Ω, in the same range as those obtained for conventional HVOF coatings (about 1.0×10^{11} Ω). After 11 days of conditioning at 97% RH the insulating resistances of the S-HVOF coatings decreased to 1.1-5.7 $\times 10^6$ Ω (4-5 orders of magnitude lower). In contrast, the values of insulating resistance for HVOF coatings after only 48 h of conditioning at 97% RH were about 3.2-3.8 $\times 10^5$ Ω, about one order of magnitude lower than those measured for the S-HVOF coatings after 11 days of conditioning at 97% RH. In very humid air the S-HVOF sprayed coatings were less sensitive to air humidity than the conventional HVOF coatings were.

3.3.2 EIS. From the EIS measurements the contributions of the resistive and capacitive components to the overall total impedance in a large frequency domain as a function of humidity could be estimated. At high frequencies the capacitive character (dielectric properties) of the impedance was predominant, whereas in the low-frequency domain the impedance was relatively independent of frequency, showing purely resistive behaviour (Fig. 6). The electrical resistance of the coatings could be determined through simple R||C equivalent circuit model fitting. The coating resistance as a function of thickness can be more conveniently expressed as the electrical resistivity $\rho = (R \cdot S)/d$, where R is the resistance (impedance), S is the surface area of the stainless steel electrode, and d is the coating thickness.

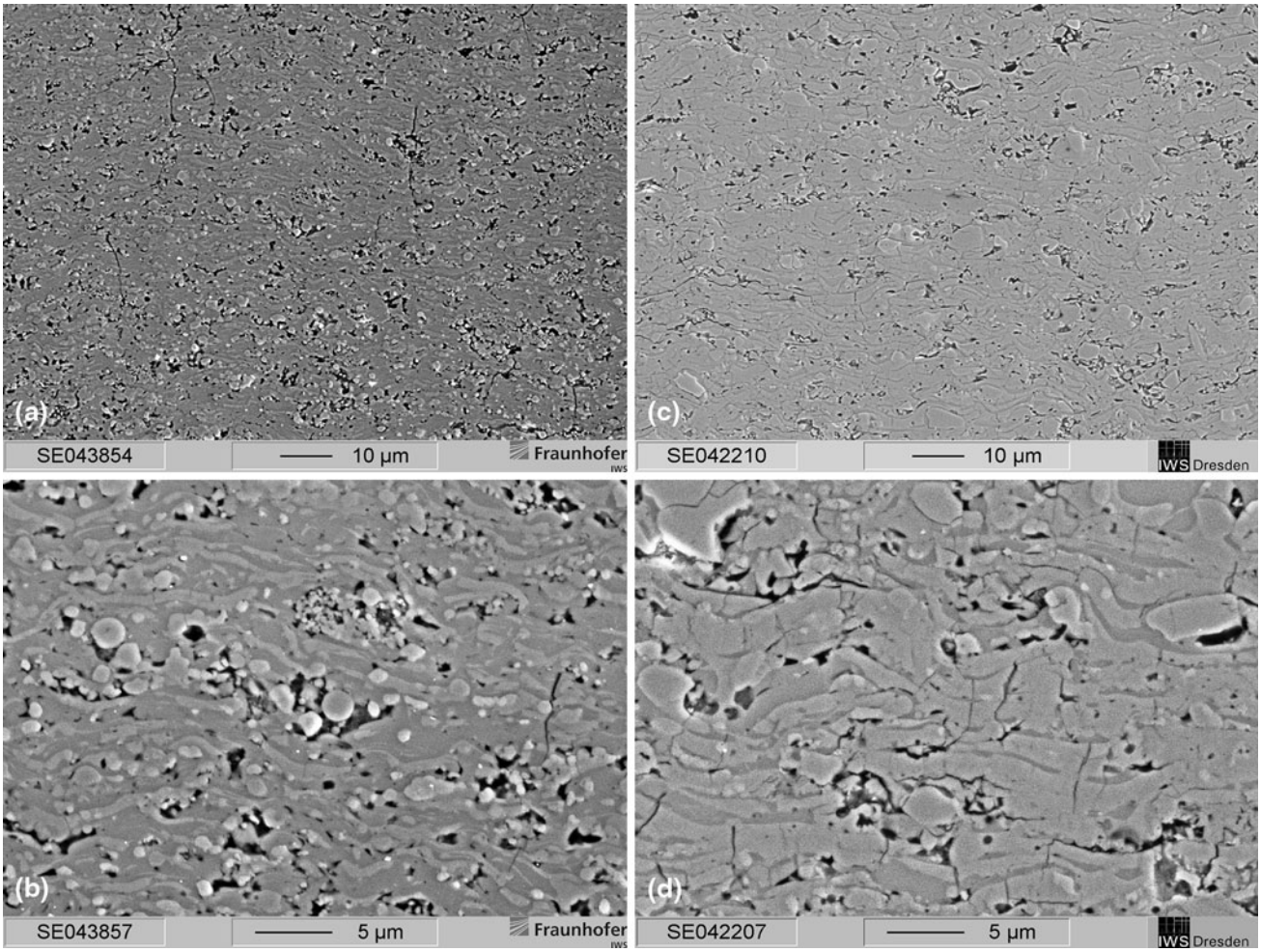

Fig. 3 SEM micrographs of cross sections of thermally sprayed coatings at different magnifications: (a and b) S-HVOF and (c and d) HVOF

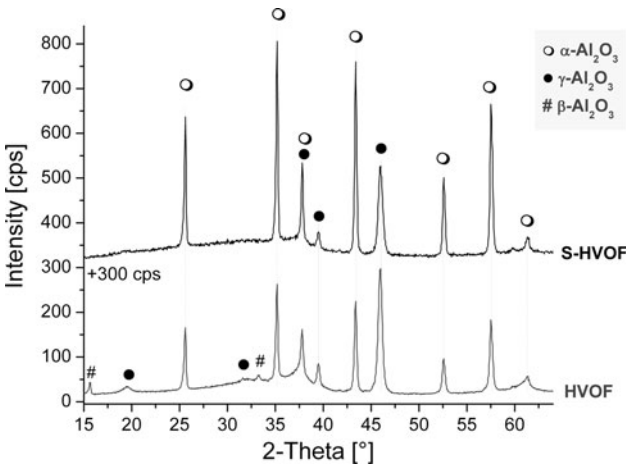

Fig. 4 XRD patterns of S-HVOF and HVOF alumina coatings

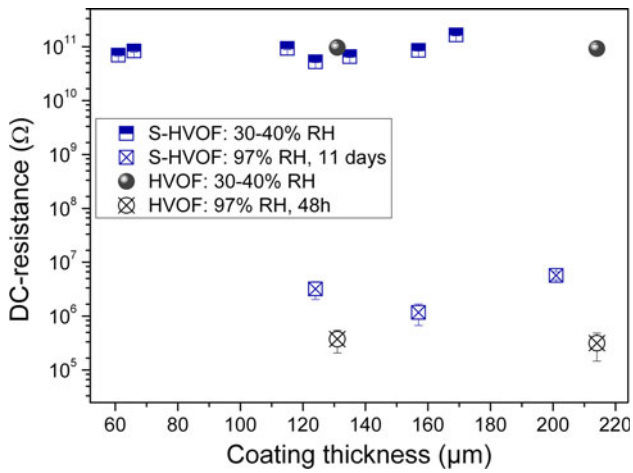

Fig. 5 DC insulating resistance as a function of coating thickness for S-HVOF and HVOF coatings in different humidity conditions (S-HVOF coatings conditioned in a desiccator at 97% RH for 11 days and HVOF coating for 48 h)

In this work only the results on electrical resistance (resistivity) are presented and discussed. The electrical resistivity behaviour of the coatings as a function of relative

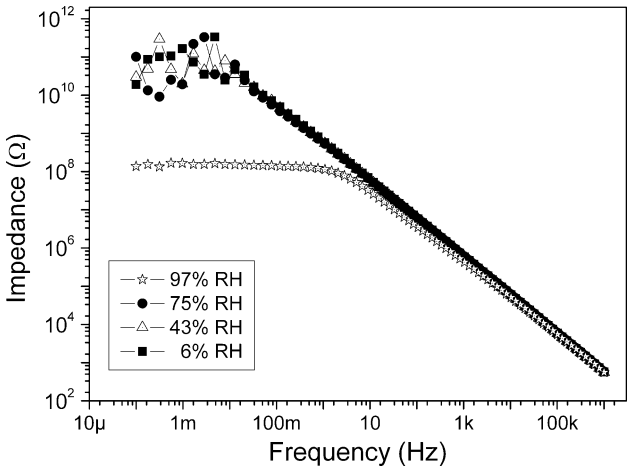

Fig. 6 Impedance as a function of frequency at different air humidity levels for a 160-µm-thick S-HVOF Al_2O_3 coating (conditioned at each RH for 86 h)

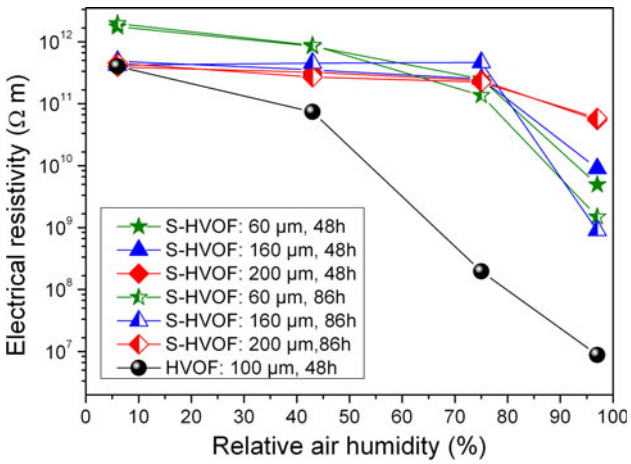

Fig. 7 Influence of the relative humidity on electrical resistivity of S-HVOF and HVOF sprayed coatings (S-HVOF coatings conditioned at different specific RH levels for 48 and 86 h and HVOF coating conditioned for 48 h)

humidity is shown in Fig. 7. The conventional HVOF coatings were conditioned for 48 h, whereas the S-HVOF coatings were tested after 48 and 86 h at each selected humidity level. In the case of conventional HVOF alumina coatings the electrical resistance (resistivity) decreased almost linearly from 4.3×10^{10} Ω (4.0×10^{11} Ω·m) at 6% RH to 9.5×10^{5} Ω (8.8×10^{6} Ω·m) at 97% RH.

After 48 h of conditioning at 6% RH values of electrical resistance (resistivity) in the range 8.1×10^{10}-1.1×10^{11} Ω (3.4×10^{11}-1.8×10^{12} Ω·m) were recorded for suspension-sprayed coatings with thicknesses from 60 to 200 µm. Comparable values were also obtained when S-HVOF coatings were conditioned for 86 h at 6% RH. The thickness of the suspension coating seemed to have little influence on the electrical properties. In the humidity range from 6% RH to 75% RH the electrical properties did not change significantly and values on the order of 10^{11} Ω·m were recorded for electrical resistivity. After 48 h of conditioning at 97% RH the electrical resistance (resistivity) of the S-HVOF coatings varied from 3.0×10^{8} Ω (4.9×10^{9} Ω·m) to 1.7×10^{10} Ω (5.4×10^{10} Ω·m), with the lower values being obtained for the thinner coating (thickness of 60 µm). The increase in duration of sample conditioning in very humid air was associated with a slight decrease in electrical properties, especially for the 60-µm-thick S-HVOF coating. Thus after 86 h of conditioning at 97% RH the resistance and resistivity decreased to 9.4×10^{7} Ω and 9.0×10^{8} Ω·m, respectively, about one order of magnitude lower than the values obtained after 48 h at the same humidity level. Nonetheless, these values were significantly higher than those recorded for the conventional coatings. At 97% RH the electrical properties were found to be up to five orders of magnitude lower for HVOF coatings and up to three orders of magnitude lower for S-HVOF coatings. Therefore according to the statement of Ivers-Tiffée and von Münch (Ref 17) that for $\rho > 10^{8}$ Ω·m the materials are considered as insulators it can be confirmed that compared with the conventional HVOF coating, the suspension sprayed coatings retained their insulating behaviour for a longer time even in environments with high relative humidities.

3.4 Dielectric Breakdown Test

The average values of DBV and dielectric strength (E_d) as a function of the kind of coating and coating thickness are shown in Fig. 8. In the case of suspension-sprayed coatings the average values of DBV increased from 1.2 to 4.0 kV when the coating thickness increased from 60 to 200 µm. A breakdown voltage up to 4.5 kV was measured for a 200-µm-thick HVOF coating. By dividing the breakdown voltage by the coating thickness the dielectric strength can be obtained. For S-HVOF coatings with thicknesses ranging from 60 to 200 µm the average values of E_d were in the range 19.5-26.8 kV·mm^{-1}. In the case of HVOF coatings E_d values were higher (up to 32 kV·mm^{-1}) than those obtained for S-HVOF coatings. However, it seemed that the dielectric strength of conventionally sprayed coatings was more sensitive to the coating thickness (when compared with the values of E_d determined for S-HVOF coatings) and varied to a greater extent (up to 10 kV·mm^{-1}) when the coating thickness varied in the range 100-200 µm. The variation in dielectric strength with coating thickness may provide additional information about the homogeneity and microstructural integrity of the coating. A lower variation in the E_d in a given thickness domain (as observed for S-HVOF coatings) should indicate a more homogeneous coating structure.

4. Discussion of Electrical Properties

4.1 Electrical Resistance: Influence of Humidity and Coating Characteristics

DC resistance tests and EIS measurements showed that under conditions of lower air humidity (up to 40% RH) the electrical properties of the alumina coatings produced by both conventional HVOF and S-HVOF processes were

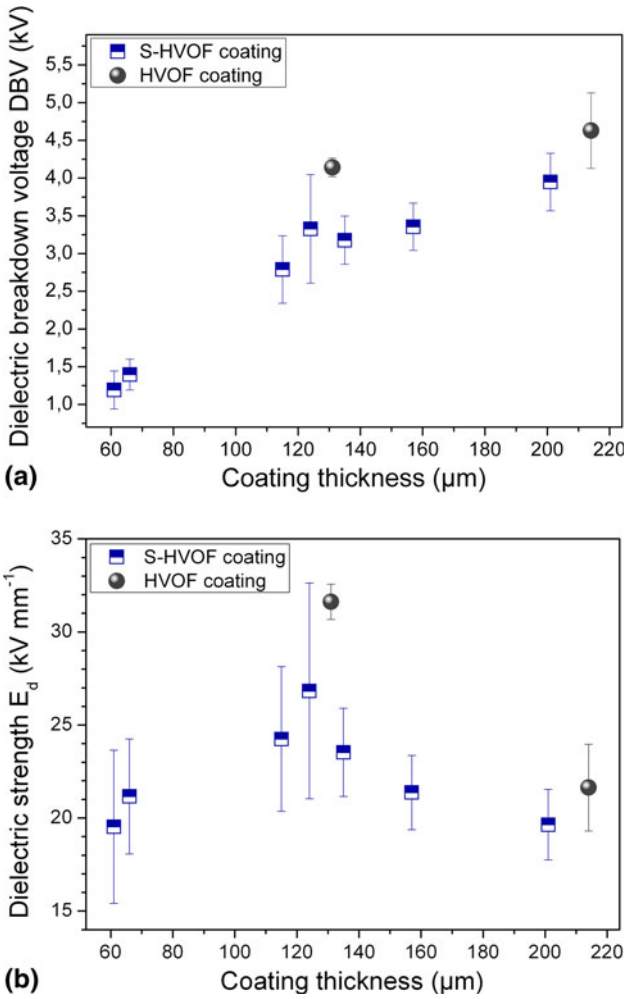

Fig. 8 Variation of dielectric properties of suspension-sprayed coatings as a function of coating thickness: (a) dielectric breakdown voltage (DBV) and (b) dielectric strength E_d

comparable. By exposing of the coatings to higher humidity levels, especially >75% RH, drastic degradation of the electrical properties was seen (Fig. 7). Moreover, significant loss of resistivity, up to six orders of magnitude, was recorded for HVOF coatings after only 48 h of exposure at 97% RH. S-HVOF coatings were less sensitive to humidity. Conditioning of suspension-sprayed coatings for 48 and 86 h at 97% RH involved a decrease in electrical properties of up to three orders of magnitude. After 11 days of conditioning at 97% RH the DC insulation resistance of the S-HVOF coatings decreased by up to five orders of magnitude, but still remained one order of magnitude higher than the DC insulation resistance of the HVOF coatings determined after only 48 h of conditioning (Fig. 5).

The deterioration of the electrical resistance with increasing humidity could be explained by the increase in the surface electrical conductivity resulting from the adsorption and accumulation of water monolayers on the surface of the oxide (Ref 8) and the capillary condensation of water in microstructural defects (cracks and open pores). As shown in the micrographs given in Fig. 3 suspension-sprayed coatings, in contrast to HVOF coatings, exhibited a specific microstructure with fewer interlamellar cracks and a significant amount of fine pores (Fig. 3a and b). The supposition that the S-HVOF coatings mainly contained closed porosity and less open or interconnected porosity was confirmed by the EIS measurements at high RH levels. S-HVOF coatings consisted mainly of α-Al_2O_3, which in humid environments is considered to be more stable than γ-Al_2O_3, although the degradation of the electrical resistance of α-Al_2O_3 powders with increasing humidity is reported (Ref 7). It can be presumed that the superior electrical properties of suspension-sprayed coatings are the result of the combined effect of the specific microstructure and the retention of a high content of α-Al_2O_3.

Besides, the presence of impurities can also affect the electrical properties of the coatings. S-HVOF coatings were produced from a powder characterised by a very high purity (>99.99%), whereas HVOF coatings were sprayed with a feedstock powder, which according to the product certification data sheet contained of about 0.13 wt.% Na_2O (see Table 1 in Ref 6). XRD analysis performed on HVOF coatings confirmed the presence of β-Al_2O_3, too. Beta-alumina is a good ionic conductor. It can be assumed that in humid environments, the presence of Na^+ ions decreases the electrical resistivity of HVOF coatings.

4.2 Dielectric Properties of the Coatings

The results of the dielectric breakdown tests indicated slightly inferior dielectric strength E_d for the S-HVOF coatings in comparison with the conventional HVOF deposits (Fig. 8b). However, more in-depth analysis of the E_d results showed that the changes in the dielectric strength of S-HVOF coatings with changing coating thickness were lower than those obtained for HVOF coatings.

The mechanism of dielectric breakdown in the sprayed coating was assumed to be more related to the coating microstructure than to the phase composition. Turunen et al. (Ref 18) proposed a correlation between the coating microstructure and nature of the pore architecture in the coating and the dielectric behaviour. Cracks, especially vertical cracks in the coating microstructure, involve the formation of the critical failure path and consequently the coating will show dielectric breakdown. Moreover, the dielectric breakdown (dielectric strength) was considered to occur through the heat/thermal mechanism (Ref 19) or electrical discharge (Ref 20-22). When an electric field was induced in the coatings the electrical resistance increased by a lesser amount than the thermal resistance of the coating did; thus heat was rapidly generated through ionic conduction, but dissipation of the heat in the coating volume was slower. It can be assumed that the presence of small pores and vertical cracks in the microstructure will enable the formation of local heating micro-zones because of the concentration of high electrical field densities, which will result in dielectric breakdown and coating damage.

As shown in the SEM micrographs given in Fig. 3(a) and (b) suspension-sprayed coatings were densely structured with none of the lamella observed in the conventional HVOF coating (Fig. 3c and d), but contained fine pores and locally distributed vertical cracks. The electrical property measurements indicated that the content, the shape and the distribution of the microstructural defects (pores and cracks) played a decisive role in determining the electrical properties of the coatings. It can be assumed that these micro-defects were 'small' enough to avoid the percolation of the water vapour in the coating, but 'big' enough to induce formation and concentration of high electrical field densities. Nonetheless, according to the values of dielectric strength determined for different coating thicknesses it can be assumed that these microstructural defects were more homogeneously distributed in the matrix of the S-HVOF coating than in the HVOF coating structure.

Supplementary investigations will be carried out in order to gain a better understanding of the relationship between the dielectric properties and the pore network architecture of the suspension-sprayed coatings.

5. Conclusions

A comparative study of the characteristics (microstructure, phase composition, and mechanical properties) and electrical properties (insulating resistance, electrical resistivity, and dielectric strength) of Al_2O_3 coatings produced by HVOF and S-HVOF processes is presented.

At low RH levels ($<40\%$ RH) the electrical resistivity was on the order of 10^{11} Ω·m for sprayed alumina coatings obtained by both conventional HVOF and S-HVOF processes. At a very high humidity (97% RH) the electrical resistivity values for the S-HVOF coatings were in the range 10^7-10^{11} Ω·m, up to five orders of magnitude higher than those recorded for the HVOF coating (10^6 Ω·m). The better electrical stability of S-HVOF coatings in highly humid environments can be explained by their specific microstructure with finer pores and lower interconnected porosity and by the retention of a high α-Al_2O_3 content. However, at very high humidities (97% RH) the electrical properties were found to degrade significantly (by up to 4-5 orders of magnitude) in these coatings after long-term exposure.

The dielectric strength of suspension-sprayed coatings was found to be 19.5-26.8 kV·mm^{-1} for coating thicknesses ranging from 60 to 200 μm. It is supposed that the coating microstructure, especially the presence of fine microstructural defects, has a greater influence on the dielectric breakdown than the phase composition does. However, further detailed study on the pore structures of the suspension-sprayed coatings and an understanding of the dielectric breakdown mechanism are necessary for this to be proven.

Acknowledgment

The authors would like to thank their colleagues at Fraunhofer IWS B. Wolf and S. Raschke for the metallographic preparation of the samples and SEM analysis and S. Saaro for assistance with XRD analysis. The results presented here are part of the BmWi-Innonet Research Project 'INNOMODUL-Innovative Aufbautechnologie für elektronische Hochleistungsmodule in Fahrzeugen durch thermisches und kinetisches Spritzen' (INNOMODUL-Innovative technology for building of high-performance electronic modules for vehicles by thermal and kinetic spraying), Project No. 16IN0695, funded by the Federal Ministry of Economics and Technology, Germany.

References

1. C.J. Swindeman, R.D. Seals, W.P. Murray, M.H. Cooper, and R.L. White, An Investigation of the Electrical Behavior of Thermally Sprayed Aluminum Oxide, *Thermal Spray: Practical Solutions for Engineering Problems*, C.C. Berndt, Ed., ASM, Materials Park, 1996, p 793-797
2. J. Takeuchi, R. Yamasaki, and Y. Harada, Development of a Low-Pressure Plasma Sprayed Ceramic Coating on Electrostatic Chucks for Semiconductor Manufacturing Equipment, *Proceedings of the International Thermal Spray Conference*, E. Lugscheider and C.C. Berndt, Eds., 4-6 Mar 2002 (Essen), DVS Verlag, Düsseldorf, 2002, p 960-964
3. C. Friedrich, R. Gadow, and A. Killinger, Thermally Sprayed Multilayer Coatings as Electrodes and Dielectrics in High Efficiency Ozoner Tubes, *Proceedings of the United Thermal Spray Conference*, E. Lugscheider, and P.A. Kammer, Eds., 17-19 Mar 1999 (Düsseldorf), DVS-German Welding Society, Düsseldorf, 1999, p 676-682
4. R. Gadow, A. Killinger, and C. Li, Plasma Sprayed Ceramic Coatings for Electrical Insulation on Glass Ceramic Components. *Proceedings of the International Thermal Spray Conference*, E. Lugscheider and C.C. Berndt, Eds., 4-6 Mar 2002 (Essen), DVS Verlag, Düsseldorf, 2002, p 213-219
5. M. Prudenziati, Development and the Implementation of High-Temperature Reliable Heaters in Plasma Spray Technology, *J. Therm. Spray Technol.*, 2008, **17**(2), p 235-243
6. F.-L. Toma, S. Scheitz, L.-M. Berger, V. Sauchuk, M. Kusnezoff, and S. Thiele, Comparative Study of the Electrical Properties and Characteristics of Thermally Sprayed Alumina and Spinel Coatings, *J. Therm. Spray Technol.*, 2011, **20**(1-2), p 195-204
7. F. Favre, F. Villieras, Y. Duval, E. McRae, and C. Rapin, Influence of Relative Humidity on Electrical Properties of α-Al_2O_3 Powders: Resistivity and Electrochemical Impedance Spectroscopy, *J. Colloid Interface Sci.*, 2005, **286**(2), p 615-620
8. B.-D. Yan, S.L. Meilink, G.W. Warren, and P. Wynblatt, Water Adsorption and Surface Conductivity Measurements on α-Alumina Substrates, *IEEE Trans. Compon. Hybrids. Manuf. Technol.*, 1987, **CHMT-10**(2), p 247-251
9. G. Bolelli, J. Rauch, V. Cannillo, A. Killinger, L. Lusvarghi, and R. Gadow, Microstructural and Tribological Investigation of High-Velocity Suspension Flame Sprayed (HVSFS) Al_2O_3 Coatings, *J. Therm. Spray Technol.*, 2009, **18**(1), p 35-49
10. F.-L. Toma, L.-M. Berger, C.C. Stahr, T. Naumann, and S. Langner, Microstructures and Functional Properties of Suspension-Sprayed Al_2O_3 and TiO_2 Coatings: An Overview, *J. Therm. Spray Technol.*, 2010, **19**(1-2), p 262-274
11. G. Darut, F. Ben-Ettouil, A. Denoirjean, G. Montavon, H. Ageorges, and P. Fauchais, Dry Sliding Behavior of Sub-Micrometer-Sized Suspension Plasma Sprayed Ceramic Oxide Coatings, *J. Therm. Spray Technol.*, 2010, **19**(1-2), p 275-285
12. G. Bolelli, V. Cannillo, R. Gadow, A. Killinger, L. Lusvarghi, J. Rauch, and M. Romagnoli, Effect of the Suspension Composition on the Microstructural Properties of High Velocity Suspension Flame Sprayed (HVSFS) Al_2O_3 Coatings, *Surf. Coat. Technol.*, 2010, **204**(8), p 1163-1179

13. F.-L. Toma, L.-M. Berger, C.C. Stahr, T. Naumann, and S. Langner, Thermisch gespritzte Al_2O_3-Schichten mit einem hohen Korundgehalt ohne eigenschaftsmindernde Zusätze und Verfahren zu ihrer Herstellung (Thermally Sprayed Al_2O_3 Coatings Having a High Content of Corundum without any Property-Reducing Additives and Method for the Production Thereof), German Patent DE 10 2008 026 101 B4 (Filing Date: 30 May 2008); EP 2300630 A1; WO 2009/146832 A1; US 2011/0123431A1; CA 2726434A1; JP 2011-522115A
14. F.-L. Toma, S. Langner, M.M. Barbosa, L.-M. Berger, C. Rödel, and A. Potthoff, Influence of the Suspension Characteristics and Spraying Parameters on the Properties of Dense Suspension-HVOF Sprayed Al_2O_3 Coatings, *Proceedings of the International Thermal Spray Conference*, 27-29 Sep 2011 (Hamburg), DVS Verlag, Düsseldorf, 2011
15. M. Barbosa, D. Schneider, R. Puschmann, F.-L. Toma, and L.-M. Berger, Microstructure Investigation of Thermally Sprayed Ceramic Coatings by Laser Acoustic Surface Waves (LAwave®) Method, *Proceedings of the International Thermal Spray Conference*, 27-29 Sep 2011 (Hamburg), DVS Verlag, Düsseldorf, 2011
16. W.C. Oliver and G.M. Pharr, Measurement of Hardness and Elastic Modulus by Instrumented Indentation: Advances in Understanding and Refinements to Methodology, *J. Mater. Res.*, 2004, **19**(1), p 3-20
17. E. Ivers-Tiffée and W. von Münch, *Werkstoffe der Elektrotechnik (Electrotechnical Materials)*, 10th ed., B.G. Teubner Verlag/GWV Fachverlage, Wiesbaden, 2007, p 142 (in German)
18. E. Turunen, T. Varis, S.-P. Hannula, A. Vaidya, A. Kulkarni, J. Gutleber, S. Sampath, and H. Herman, On the Role of Particle State and Deposition Procedure on Mechanical, Tribological and Dielectric Response of High Velocity Oxy-Fuel Sprayed Alumina Coatings, *Mater. Sci. Eng. A*, 2006, **415**(1-2), p 1-11
19. H.-J. Kim, S. Odoul, C.-H. Lee, and Y.-G. Kweon, The Electrical Insulation Behaviour and Sealing Effects of Plasma Sprayed Alumina-Titania Coatings, *Surf. Coat. Technol.*, 2001, **140**(3), p 293-301
20. F. Hövelmann, Hochspannungstechnik-Elektrische Festigkeit Teil 2: Durchschlag gasförmiger, flüssiger und fester Isolierstoffe, Fernstudienbrückenkurse: Studiengang Elektrische Energietechnik 1, Technische Fachhochschule, Berlin, 1993 (in German)
21. E. Rajamäki, T. Varis, A. Kulkarni, A.J. Gutleber, A. Vaidya, M. Karadge, S. Sampath, and H. Herman, Parameter Optimization of HVOF Sprayed Alumina and Effect of the Spray Parameters on the Electrical Properties of the Coatings, *Proceedings of the International Thermal Spray Conference*, E. Lugscheider and C.C. Berndt, Eds., 4-6 Mar 2002 (Essen), DVS Verlag, Düsseldorf, 2002, p 622-626
22. C.T. Morse and G.J. Hill, The Electric Strength of Alumina: The Effect of Porosity, *Proc. Br. Ceram. Soc.*, 1970, **180**, p 23-35